Patterning metamaterials for fast and efficient single-photon sources

O. A. Makarova, M. Y. Shalaginov, S. Bogdanov, U. Guler,
A. Boltasseva, A. V. Kildishev, and V. M. Shalaev*
School of Electrical & Computer Engineering, Birck Nanotechnology Center, and
Purdue Quantum Center, Purdue University, West Lafayette, IN 47907, USA
*shalaev@purdue.edu

ABSTRACT

Solid state quantum emitters are prime candidates to realize fast on-demand single-photon sources. The improvement in photon emission and collection efficiencies for quantum emitters, such as nitrogen-vacancy (NV) centers in diamond, can be achieved by using a near-field coupling to nanophotonic structures. Plasmonic metamaterial structures with hyperbolic dispersion have been previously demonstrated to significantly increase the fluorescence decay rates from NV centers. However, the electromagnetic waves propagating inside the metamaterial must be outcoupled before they succumb to ohmic losses. We propose a nano-grooved hyperbolic metamaterial that improves the collection efficiency from a nanodiamond-based NV center by a factor of 4.3 compared to the case of coupling to a flat metamaterial. Our design can be utilized to achieve highly efficient and fast single-photon sources based on a variety of quantum emitters.

Keywords: single-photon source, hyperbolic metamaterials, nanopatterning

1. INTRODUCTION

Efficient generation of single photons is important for applications in quantum information such as quantum computation [1], quantum key distribution [2] and transfer of quantum information [3]. Ideally, such a source must produce one and only one photon on demand with an arbitrarily fast repetition rate, emitting into a specific mode or direction. Integrated single-photon sources (SPS) have been demonstrated based on different emitters, including crystallographic defects in diamond [4–8], SiC [9], ZnO [10] and 2D materials [11], quantum dots [12], and carbon nanotubes [13].

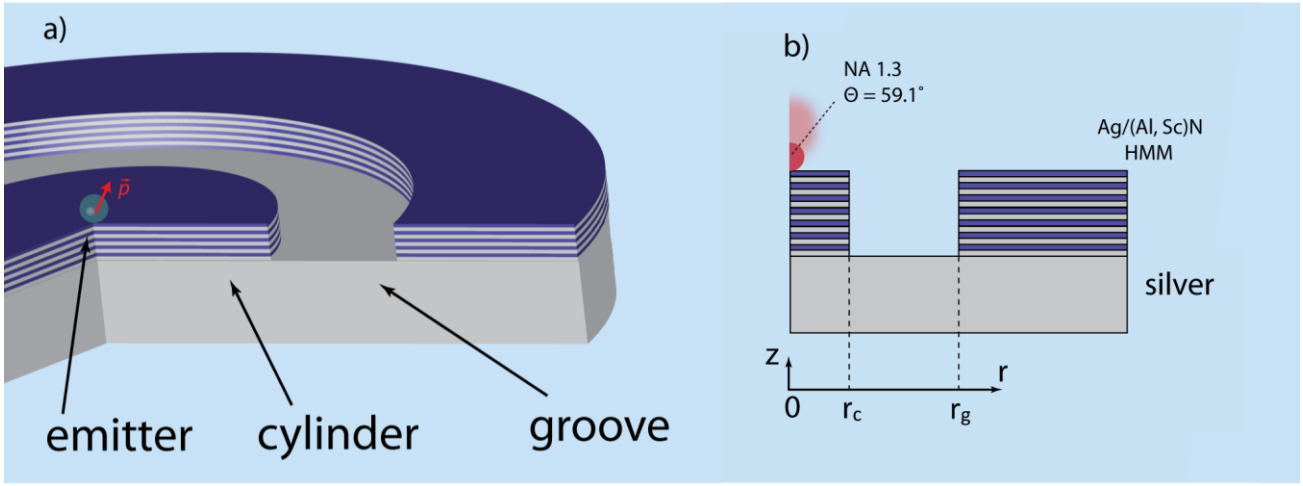

Figure 1. a) The geometry of an emitter and outcoupling structure. b) Collection efficiency is calculated for an oil-immersion objective with NA 1.3 (corresponding collection angle 59.1°).

Numerous applications in quantum communications, such as secure key distribution and large cluster states generation, demand availability of deterministically controlled SPS. Deterministic single photon operation can be achieved by combining together ultra-fast response of the emitter on external trigger with efficient collection of the emitted signal. The

improvement in photon emission and collection efficiencies for quantum emitters can be achieved by near-field coupling to nanophotonic structures [14–20]. In the case of room-temperature emitters operating at different wavelengths, a resonance approach may not fit well, since tuning the cavity resonances for each particular emitter is technologically challenging.

Metamaterials with hyperbolic dispersion, so called hyperbolic metamaterials (HMM), can provide an arbitrary large photonic density of states in a broad wavelength range. Hence, near field coupling of SPS will lead to significant broadband enhancement of emission rate [21–23]. However, previous experimental studies of emitters on planar HMMs [24–26] showed that the power emitted by an SPS, which is released in the form of propagating plasmonic waves inside of the HMM, is eventually dissipated inside the metamaterial due to ohmic losses. The HMM surface patterning can scatter the propagating HMM waves and redirect them into the far field, hence significantly improving the photon collection efficiency [27–30]. In this work, we propose a simple nanostructure made of HMM, which is expected to improve the collection efficiency up to 40% over a broad wavelength range.

The proposed design is based on a circular groove milled in a planar lamellar HMM deposited on a metal substrate (see Fig. 1a). We analyze the scattering performance depending on dipole orientation and wavelength of the emission. The planar HMM with a circular groove structure consistently outperforms the same planar HMM without groves demonstrating both higher collection efficiency (β) and Purcell factor (PF). The optimization was performed to achieve the maximum value of these values. The planar HMM under test consists of 8 pairs of layers, with layer thicknesses being t_{Ag} = 10 nm and $t_{(Al, Sc)N}$ = 20 nm for Ag and (Al, Sc)N, respectively, resulting in a total thickness of t_{HMM} = 240 nm. The outcoupling structure involves three regions created by the groove: a central HMM cylinder ($0 < r < r_c$), a circular groove itself ($r_c \leq r \leq r_g$), and an exterior HMM region ($r_g < r$). The emitter is placed at r = 0 above the HMM surface. The wavelength for optimizing the PF and collection efficiency was chosen to be 685 nm. For the emitter with averaged orientation, 4-fold improvement in collection efficiency and emission directionality is predicted over the broad emission spectrum (600-800nm) relative to an emitter on the planar HMM with no groove. Although in our studies, we have chosen a nitrogen-vacancy (NV) in the center of a 50-nm nanodiamond as an example of a room temperature solid-state SPS, the findings of our work can be extended to a broader family of similar emitters.

2. METHODS

The HMM was modeled as a superlattice of alternating ultrathin metal (Ag) and dielectric layers ((Al, Sc)N). Ag has been chosen as a material with the lowest losses and (Al, Sc)N as a dielectric material which can lattice match Ag. We consider the Ag/(Al, Sc)N epitaxially grown superlattice to demonstrate the best HMM performance due to low intrinsic material losses, ultra-thin layers, and smooth interfaces between the layers. The proposed superlattice can be in principle fabricated adopting the technique described in Ref [31]. The Ag - (Al,Sc)N HMM promises to have smooth layers of defined thickness and be more suitable for patterning. An immersion oil was taken for superstrate and silver for substrate.

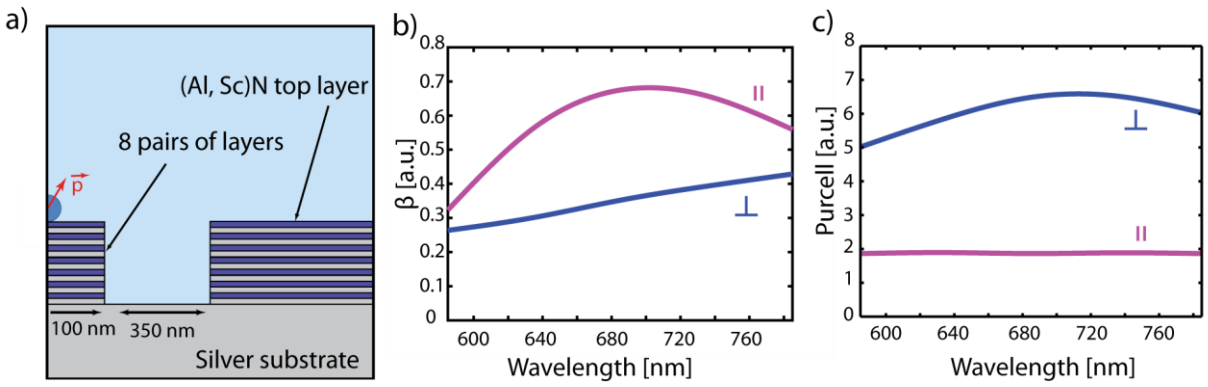

Figure 2. a) Geometry of the optimized outcoupling structure. b) The ratio of the collected and total emitted powers for perpendicular (⊥) and radial (∥) orientations. c) Broadband behavior of the Purcell factor [a.u.].

The main goal of the optimization was to achieve the maximum value of collection efficiency (β) along with the highest Purcell factor (PF). Numerical simulations were performed using finite-element method using a commercial solver (COMSOL Multiphysics, Wave Optics Module). In the simulations, we approximated an NV center as an electric dipole, implemented as external current density in a 2-nm-diameter sphere. The dipolar emitter is located in the center of a diamond sphere with a radius of 25 nm. The totally dissipated power was computed as an integral of power flux through the 6-nm-radius sphere surrounding the emitter. The objective collected power was defined as if it would be collected by a microscope objective with 1.3 numerical aperture. Obtained for power results were normalized for an emission from the same source in a vacuum. The emission enhancement study was separated for different dipoles orientations, such as radial (∥, along the r-axis) and perpendicular to the substrate (⊥, along the z-axis). Statistically averaged PF and β are calculated as a normalized sum of power contributions from a perpendicular and in-plane dipole orientations correspondingly multiplied by factors of 1/3 and 2/3. Based on these values, objective collection efficiency was calculated as a ratio of collected and total radiated powers. The corner of the cylinder is predicted to work as an outcoupler for the propagating inside of the material modes, while the border of the outside region could allow the formation of a photonic cavity. By changing the radius of the cylinder, it is possible to change the number of metamaterial modes and their ability of reaching the corner of the cylinder for outcoupling into the free-space. Metal as a substrate material is proposed to act as a mirror and prevent the mode propagation inside the material.

The optimization was performed by sweeping values of one parameter while keeping others intact. The optimal parameter value obtained from each sweep was utilized as a constant for the optimization of the next parameter. Investigated parameters included central cylinder radius, groove width, pairs of layers number, vertical emitter position relative to the structure surface, the top layer (Ag or (Al, Sc)N), and substrate material (Ag or MgO). The optimization was performed for the wavelength of 685 nm. The ⊥ orientation appeared to be more sensitive to the parameters change, so it was used for a finer choice of the value. The fully optimized parameters are presented in Figure 2a and the resulting spectra of β and PF are shown in Figure 2 b and c, respectively. Collection efficiency β was higher for IP orientation, while a larger PF was predicted for ⊥ dipole.

3. RESULTS

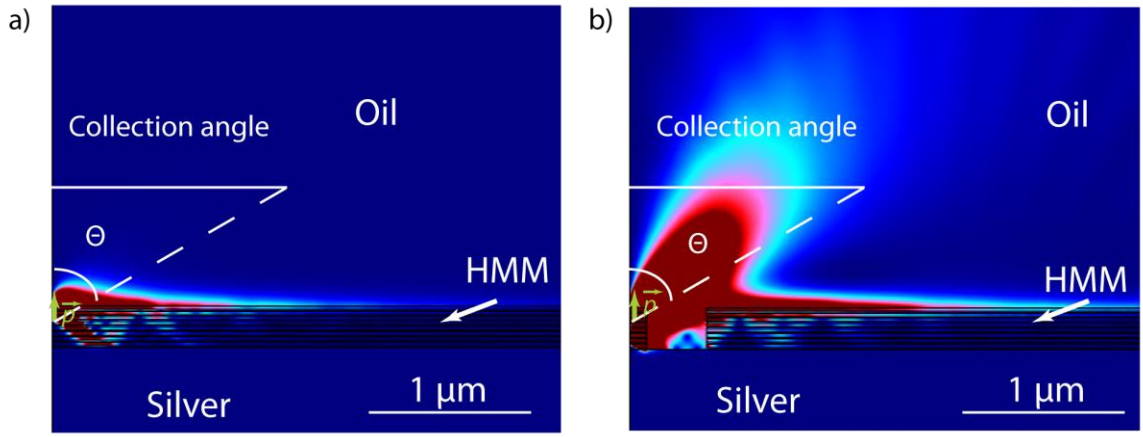

Figure 3. Power density distribution for a perpendicular dipole on a) planar HMM ($r_c \to \infty$) and b) optimally patterned HMM. The structure allows outcoupling at the cylinder corner resulting in the increase of collected power by a factor of 50 for 685 nm emission wavelength.

First, we considered the dipole oriented along the z-axis perpendicular to the metamaterial layers (⊥). Such emitter experiences the strongest coupling to metamaterial modes, resulting in less than 1% of the total emitted power collection (Fig. 3a) as most of the emission gets lost inside of the material. At the wavelength of study (685 nm), we observed an increase in the collected power by up to a factor of 50, compared to the case of a planar HMM ($r_c \to \infty$). This improvement is mostly caused by a 40-fold increase in β, due to scattering of modes propagating inside the HMM at cylinder corners ($r = r_c$) and their outcoupling into free space (Fig. 3b). Variation of the cylinder radius allowed to find the ideal parameter to outcouple sufficient amount of propagating modes.

For the radial dipole orientation (∥) unpatterned planar HMM acts as a mirror resulting in collection efficiency of 15%. In the case of patterned HMM, the exterior edge of the groove ($r = r_g$) forms a weak cavity for plasmonic and photonic waves (Fig. 4). This effect additionally increases β by a factor of 1.5 comparing to the case without the exterior edge ($r_g \to \infty$). The collection efficiency at 685 nm increases from 15% to almost 70%, resulting in total collected power improvement by a factor of 2.4.

The optimally patterned structure predicts a good broadband performance with improvement in total collected power by a factor of 4 and collection efficiency of 42%. The effect of the modes scattering gives a constantly high β for ⊥ emitter at all studied wavelengths. The photonic cavity formed by the exterior edge of the groove for the IP-oriented emitter works best for the emission maximum wavelength but features an improvement across the whole spectrum.

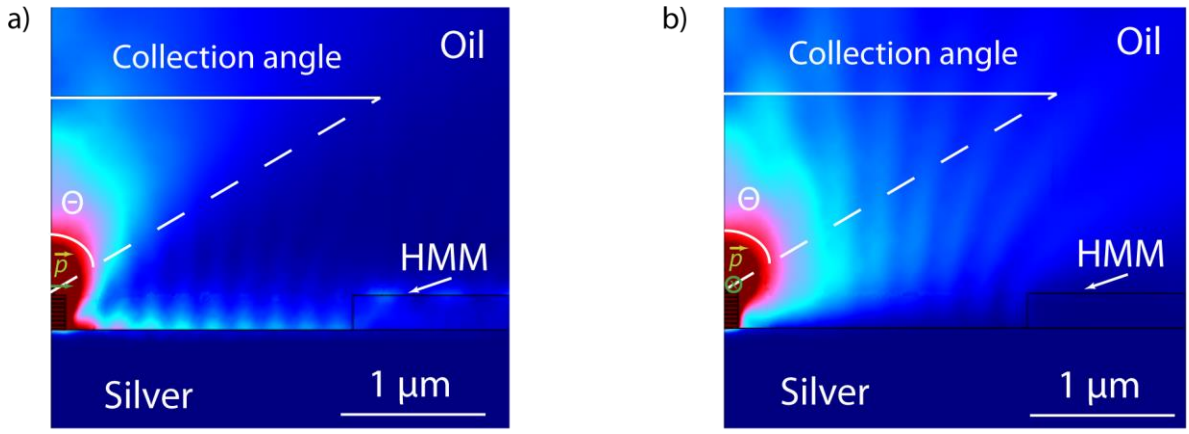

Figure 4. Power density distribution for in-plane (a) and out-of-plane (b) radial dipole emitter (green arrows) placed on top of HMM with a 2-μm groove. The groove exterior edge reflects surface plasmon-polariton (a) and photonic waves (b) resulting in extra contribution to the collection efficiency.

4. CONCLUSION AND OUTLOOK

Quantum emitters coupled to hyperbolic metamaterials constitute a viable approach to fast and efficient single-photon sources. Tailored patterning of an HMM surface significantly enhances the collection efficiency from quantum emitters in a broad wavelength range and all dipole orientations, constituting a robust device design with high potential for room-temperature applications. To achieve efficient collection of radiation, a single groove is needed, which can be relatively simply achieved with modern nanofabrication tools. The groove leads to a 50-fold increase in objective coupling efficiency for the out of plane oriented dipole at the wavelength of the emission maximum compared to an emitter on the planar metamaterial. When both dipole orientation and emission wavelength (600-800 nm) are averaged out, the structure promises 43% objective coupling efficiency and the total increase in the collected power by a factor of 4 compared to an unpatterned HMM.

These results can be experimentally verified using room-temperature NV centers in nanodiamonds, with emission band within the presented range. It has been previously shown that structural defects in planar HMMs could significantly enhance HMM mode outcoupling from such broadband emitters [26]. Our design offers a deterministic approach that promises an even better collection for a configuration that could be realized in a scalable manner.

ACKNOWLEDGEMENTS

This work is supported by National Science Foundation (NSF) MRSEC (DMR-1120923) and ONR grant (N00014-13-1-0649). The authors would like to thank Alexey Akimov, Vadim Vorobyov, Stepan Bolshedvorskii, Vladimir Soshenko, and Vadim Kovalyuk for fruitful discussions.

REFERENCES

1. P. Kok, W. J. Munro, K. Nemoto, T. C. Ralph, J. P. Dowling, and G. J. Milburn, "Linear optical quantum computing with photonic qubits," Rev. Mod. Phys. **79**, 135–174 (2007).
2. M. Leifgen, T. Schröder, F. Gädeke, R. Riemann, V. Métillon, E. Neu, C. Hepp, C. Arend, C. Becher, K. Lauritsen, and O. Benson, "Evaluation of nitrogen- and silicon-vacancy defect centres as single photon sources in quantum key distribution," New J. Phys. **16**, 23021 (2014).
3. H. J. Kimble, "The quantum internet," Nature **453**, 1023–1030 (2008).
4. R. Albrecht, A. Bommer, C. Deutsch, J. Reichel, and C. Becher, "Coupling of a Single Nitrogen-Vacancy Center in Diamond to a Fiber-Based Microcavity," Phys. Rev. Lett. **110**, 243602 (2013).
5. T. Schröder, F. Gädeke, M. J. Banholzer, and O. Benson, "Ultrabright and efficient single-photon generation based on nitrogen-vacancy centres in nanodiamonds on a solid immersion lens," New J. Phys. **13**, 55017 (2011).
6. E. Neu, D. Steinmetz, J. Riedrich-Möller, S. Gsell, M. Fischer, M. Schreck, and C. Becher, "Single photon emission from silicon-vacancy colour centres in chemical vapour deposition nano-diamonds on iridium," New J. Phys. **13**, 25012 (2011).
7. A. Sipahigil, K. D. Jahnke, L. J. Rogers, T. Teraji, J. Isoya, A. S. Zibrov, F. Jelezko, and M. D. Lukin, "Indistinguishable photons from separated silicon-vacancy centers in diamond," Phys. Rev. Lett. **113**, 1–5 (2014).
8. I. Aharonovich, D. Englund, and M. Toth, "Solid-state single-photon emitters," Nat. Photonics **10**, 631–641 (2016).
9. A. L. Falk, B. B. Buckley, G. Calusine, W. F. Koehl, V. V Dobrovitski, A. Politi, C. A. Zorman, P. X. Feng, and D. D. Awschalom, "Polytype control of spin qubits in silicon carbide," Nat. Commun. **4**, 1–7 (2013).
10. A. J. Morfa, B. C. Gibson, M. Karg, T. J. Karle, A. D. Greentree, P. Mulvaney, and S. Tomljenovic-Hanic, "Single-Photon Emission and Quantum Characterization of Zinc Oxide Defects," Nano Lett. **12**, 949–954 (2012).
11. Y.-M. He, G. Clark, J. R. Schaibley, Y. He, M. Chen, Y. Wei, X. Ding, Q. Zhang, W. Yao, X. Xu, C. Lu, and J. Pan, "Single quantum emitters in monolayer semiconductors," Nat. Nanotechnol. **10**, 497–502 (2015).
12. J. Claudon, J. Bleuse, N. S. Malik, M. Bazin, P. Jaffrennou, N. Gregersen, C. Sauvan, P. Lalanne, and J.-M. Gérard, "A highly efficient single-photon source based on a quantum dot in a photonic nanowire," Nat. Photonics **4**, 174–177 (2010).
13. S. Khasminskaya, F. Pyatkov, K. Słowik, S. Ferrari, O. Kahl, V. Kovalyuk, P. Rath, A. Vetter, F. Hennrich, M. M. Kappes, G. Gol'tsman, A. Korneev, C. Rockstuhl, R. Krupke, and W. H. P. Pernice, "Fully integrated quantum photonic circuit with an electrically driven light source," Nature **to be publ**, 1–19 (2016).
14. E. Bermúdez-Ureña, C. Gonzalez-Ballestero, M. Geiselmann, R. Marty, I. P. Radko, T. Holmgaard, Y. Alaverdyan, E. Moreno, F. J. García-Vidal, S. I. Bozhevolnyi, and R. Quidant, "Coupling of individual quantum emitters to channel plasmons," Nat. Commun. **6**, 7883 (2015).
15. J. T. Choy, I. Bulu, B. J. M. Hausmann, E. Janitz, I. Huang, and M. Lončar, "Spontaneous emission and collection efficiency enhancement of single emitters in diamond via plasmonic cavities and gratings," Appl. Phys. Lett. **103**, 161101 (2013).
16. G. M. Akselrod, C. Argyropoulos, T. B. Hoang, C. Ciracì, C. Fang, J. Huang, D. R. Smith, and M. H. Mikkelsen, "Probing the mechanisms of large Purcell enhancement in plasmonic nanoantennas," Nat. Photonics **8**, 835–840 (2014).
17. D. Englund, B. Shields, K. Rivoire, F. Hatami, J. Vučković, H. Park, and M. D. Lukin, "Deterministic Coupling of a Single Nitrogen Vacancy Center to a Photonic Crystal Cavity," Nano Lett. **10**, 3922–3926 (2010).

18. J. Riedrich-Möller, L. Kipfstuhl, C. Hepp, E. Neu, C. Pauly, F. Mücklich, A. Baur, M. Wandt, S. Wolff, M. Fischer, S. Gsell, M. Schreck, and C. Becher, "One- and two-dimensional photonic crystal microcavities in single crystal diamond.," Nat. Nanotechnol. **7**, 69–74 (2012).

19. M. L. Andersen, S. Stobbe, A. S. Sørensen, and P. Lodahl, "Strongly Modified Plasmon-Matter Interaction with Mesoscopic Quantum Emitters," Nat. Phys. **7**, 215–218 (2011).

20. A. G. Curto, G. Volpe, T. H. Taminiau, M. P. Kreuzer, R. Quidant, and N. F. van Hulst, "Unidirectional Emission of a Quantum Dot Coupled to a Nanoantenna," Science (80-.). **329**, 930–933 (2010).

21. Z. Jacob, I. I. Smolyaninov, and E. E. Narimanov, "Broadband Purcell effect: Radiative decay engineering with metamaterials," Appl. Phys. Lett. **100**, 181105 (2012).

22. L. Ferrari, C. Wu, and D. Lepage, "Hyperbolic metamaterials and their applications," Prog. Quantum Electron. **40**, 1–40 (2015).

23. C. L. Cortes, W. Newman, S. Molesky, and Z. Jacob, "Corrigendum: Quantum nanophotonics using hyperbolic metamaterials (2012 J. Opt. 14 063001)," J. Opt. **16**, 129501 (2014).

24. M. A. Noginov, H. Li, Y. A. Barnakov, D. Dryden, G. Nataraj, G. Zhu, C. E. Bonner, M. Mayy, Z. Jacob, and E. E. Narimanov, "Controlling spontaneous emission with metamaterials," Opt. Lett. **35**, 1863 (2010).

25. J. Kim, V. P. Drachev, Z. Jacob, G. V. Naik, A. Boltasseva, E. E. Narimanov, and V. M. Shalaev, "Improving the radiative decay rate for dye molecules with hyperbolic metamaterials," Opt. Express **20**, 8100 (2012).

26. M. Y. Shalaginov, V. V. Vorobyov, J. Liu, M. Ferrera, A. V. Akimov, A. Lagutchev, A. N. Smolyaninov, V. V. Klimov, J. Irudayaraj, A. V. Kildishev, A. Boltasseva, and V. M. Shalaev, "Enhancement of single-photon emission from nitrogen-vacancy centers with TiN/(Al,Sc)N hyperbolic metamaterial," Laser Photon. Rev. **9**, 120–127 (2015).

27. T. Galfsky, H. N. S. Krishnamoorthy, W. Newman, E. E. Narimanov, Z. Jacob, and V. M. Menon, "Active hyperbolic metamaterials: enhanced spontaneous emission and light extraction," Optica **2**, 62 (2015).

28. T. Galfsky, Z. Sun, C. R. Considine, C. Chou, W. Ko, Y. Lee, E. E. Narimanov, and V. M. Menon, "Broadband Enhancement of Spontaneous Emission in Two-Dimensional Semiconductors Using Photonic Hypercrystals," Nano Lett. **16**, 4940–4945 (2016).

29. D. Lu, J. J. Kan, E. E. Fullerton, and Z. Liu, "Enhancing spontaneous emission rates of molecules using nanopatterned multilayer hyperbolic metamaterials," Nat. Nanotechnol. **9**, 48–53 (2014).

30. C. Guclu, T. S. Luk, G. T. Wang, and F. Capolino, "Radiative emission enhancement using nano-antennas made of hyperbolic metamaterial resonators," Appl. Phys. Lett. **105**, 123101 (2014).

31. B. Saha, S. Saber, G. V. Naik, A. Boltasseva, E. A. Stach, E. P. Kvam, and T. D. Sands, "Development of epitaxial Al x Sc 1− x N for artificially structured metal/semiconductor superlattice metamaterials," Phys. status solidi **252**, 251–259 (2015).